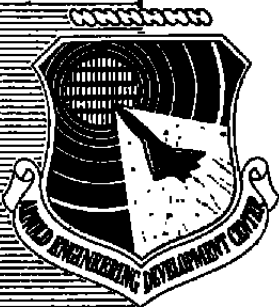# A VORTEX LATTICE TECHNIQUE FOR COMPUTING VENTILATED WIND TUNNEL WALL INTERFERENCE

F. L. Heltsley and W. E. Dietz, Jr.
ARO, Inc., a Sverdrup Corporation Company

PROPULSION WIND TUNNEL FACILITY
ARNOLD ENGINEERING DEVELOPMENT CENTER
AIR FORCE SYSTEMS COMMAND
ARNOLD AIR FORCE STATION, TENNESSEE 37389

June 1979

Final Report for Period January 1976 — September 1977

Prepared for

NASA/AMES RESEARCH CENTER
MOFFETT FIELD, CALIFORNIA 94035

NOTICES

When U. S. Government drawings, specifications, or other data are used for any purpose other than a definitely related Government procurement operation, the Government thereby incurs no responsibility nor any obligation whatsoever, and the fact that the Government may have formulated, furnished, or in any way supplied the said drawings, specifications, or other data, is not to be regarded by implication or otherwise, or in any manner licensing the holder or any other person or corporation, or conveying any rights or permission to manufacture, use, or sell any patented invention that may in any way be related thereto.
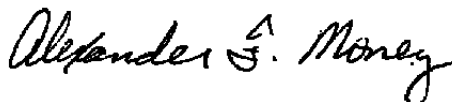
Qualified users may obtain copies of this report from the Defense Documentation Center.

References to named commerical products in this report are not to be considered in any sense as an indorsement of the product by the United States Air Force or the Government.

This report has been reviewed by the Information Office (OI) and is releasable to the National Technical Information Service (NTIS). At NTIS, it will be available to the general public, including foreign nations.

APPROVAL STATEMENT

This report has been reviewed and approved.

ALEXANDER F. MONEY
Project Manager, Research Division
Directorate of Test Engineering

Approved for publication:

FOR THE COMMANDER

ROBERT W. CROSSLEY, Lt Colonel, USAF
Acting Director of Test Engineering
Deputy for Operations

REPORT DOCUMENTATION PAGE		READ INSTRUCTIONS BEFORE COMPLETING FORM
1. REPORT NUMBER AEDC-TR-79-21	2 GOVT ACCESSION NO.	3. RECIPIENT'S CATALOG NUMBER
4. TITLE (and Subtitle) A VORTEX LATTICE TECHNIQUE FOR COMPUTING VENTILATED WIND TUNNEL WALL INTERFERENCE		5. TYPE OF REPORT & PERIOD COVERED Final Report, Jan 1976-Sept 1977
		6. PERFORMING ORG. REPORT NUMBER
7. AUTHOR(s) F. L. Heltsley and W. E. Dietz, Jr., ARO, Inc., a Sverdrup Corporation Company		8. CONTRACT OR GRANT NUMBER(s) .
9. PERFORMING ORGANIZATION NAME AND ADDRESS Arnold Engineering Development Center Air Force Systems Command Arnold Air Force Station, TN 37389		10. PROGRAM ELEMENT, PROJECT, TASK AREA & WORK UNIT NUMBERS Program Element 921E07
11. CONTROLLING OFFICE NAME AND ADDRESS NASA/Ames Research Center Moffett Field, CA 94035		12. REPORT DATE June 1979
		13. NUMBER OF PAGES 28
14. MONITORING AGENCY NAME & ADDRESS(if different from Controlling Office)		15. SECURITY CLASS. (of this report) UNCLASSIFIED
		15a. DECLASSIFICATION/DOWNGRADING SCHEDULE N/A

16. DISTRIBUTION STATEMENT (of this Report)

Approved for public release; distribution unlimited.

17. DISTRIBUTION STATEMENT (of the abstract entered in Block 20, if different from Report)

18. SUPPLEMENTARY NOTES

Available in DDC.

19. KEY WORDS (Continue on reverse side if necessary and identify by block number)

interference	rates
walls	vortices
wind tunnels	
detectors	

20. ABSTRACT (Continue on reverse side if necessary and identify by block number)

A vortex lattice method has been applied to the problem of predicting the interference induced by ventilated wind tunnel walls. The formulations of both perforated and slotted wall boundaries using the vortex lattice method are presented. Wall interference effects on a single lifting line vortex for several basic wind tunnel test section configurations are compared with other theoretical results. Use of the vortex lattice method to calculate the aerodynamic characteristics of a lifting model too

DD FORM 1 JAN 73 1473 EDITION OF 1 NOV 65 IS OBSOLETE

20. ABSTRACT, Concluded

complex for exact analytical treatment is discussed. The surface pressure distribution on a combined wing and tail representation computed for a free stream is presented as well as those for both closed and slotted test sections to illustrate the capability of the technique.

AFSC
Arnold AFS Tenn

PREFACE

The work reported herein was conducted by the Arnold Engineering Development Center (AEDC), Air Force Systems Command (AFSC), at the request of NASA/Ames Research Center, Moffett Field, California. The results of the research were obtained by ARO, Inc., AEDC Division (a Sverdrup Corporation Company), operating contractor for the AEDC, AFSC, Arnold Air Force Station, Tennessee, under ARO Project Numbers P34A-C3A and P34A-K8A. The NASA/Ames project manager was Mr. Kenneth W. Mort. The manuscript was submitted for publication on March 6, 1979.

CONTENTS

ILLUSTRATIONS

1.0 INTRODUCTION

The usual methods of calculation of wind tunnel wall interference (as discussed in Refs. 1 through 10) are generally unsatisfactory for those cases where extreme downwash is required for lift generation, such as for VSTOL configurations. A study was conducted to evaluate the vortex lattice technique as a tool for the calculation of wind tunnel wall interference. Vortex lattice simulations were formulated for closed wind tunnel walls and for both perforated and slotted boundary conditions. Solutions were obtained for selected basic tunnel configurations and were compared with results from other available theoretical techniques. In addition, solutions for a more complex wind tunnel/lifting model combination were computed to demonstrate the ability to calculate interference for configurations for which no exact analytic solution is feasible.

2.0 VORTEX LATTICE FORMULATION

The vortex lattice technique is a numerical method for solving the three-dimensional Laplace equation. A computer program recently developed at AEDC is capable of representing complex arbitrary shapes such as the one illustrated in Fig. 1, from Ref. 11. The program can calculate velocities and pressure coefficients, both on the body surface and in the flow field. Streamlines and contour plots or parameters such as flow angularity, pressure coefficient, etc. are also available.

The program was adapted to compute the classical lift interference factor, δ, defined in Ref. 1 as

$$\delta = \left(C/S\, C_L \right) \left(w/V_\infty \right) \tag{1}$$

Results were found to correlate well with solutions for several basic closed wall tunnel configurations (Refs. 1 and 4). For example, the distribution of interference along the test section centerline for a single horseshoe vortex is presented in Fig. 2 for four tunnel cross sections. Included is the distribution of interference computed using the vortex lattice representation of the NASA/Ames 40- by 80-ft flat oval wind tunnel shown in Fig. 3. A modified interference factor, δ', has been used to illustrate the effect of cross-sectional area as well as shape. The factor, defined as

$$\delta' = \delta C'/C \tag{2}$$

relates the interference of each tunnel to that of a square test section having a cross-sectional area, C'.
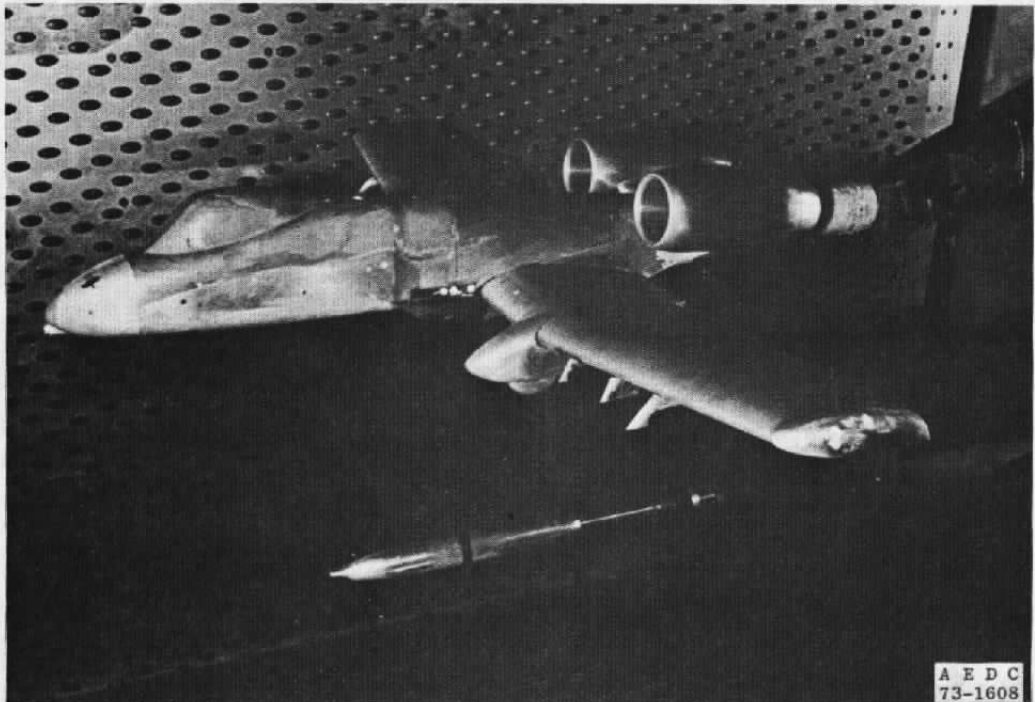
a. Wind tunnel model installation

Side View

Bottom View
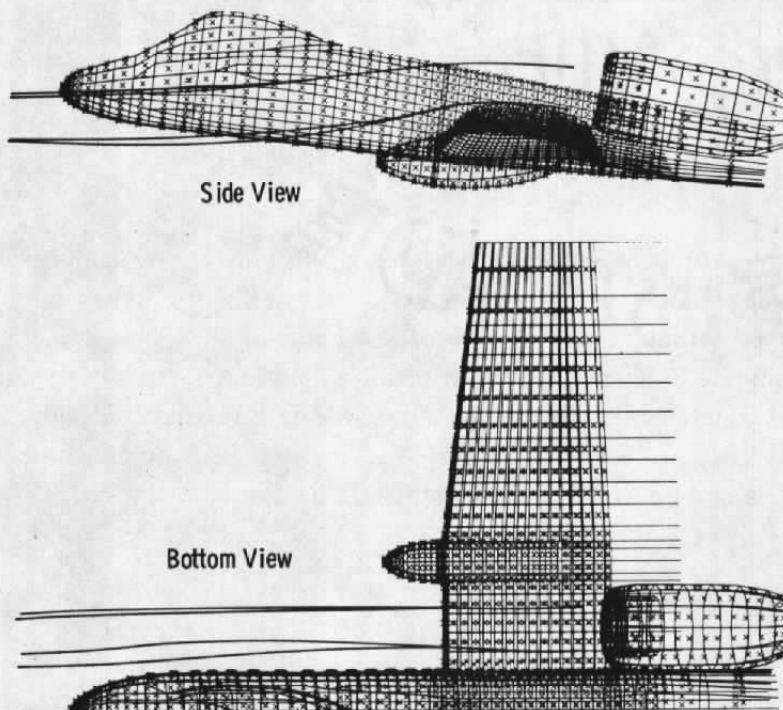
b. Vortex lattice representation
Figure 1. Typical application of the vortex lattice technique.

6

Figure 2. Theoretical wall interference for several closed tunnel cross sections.

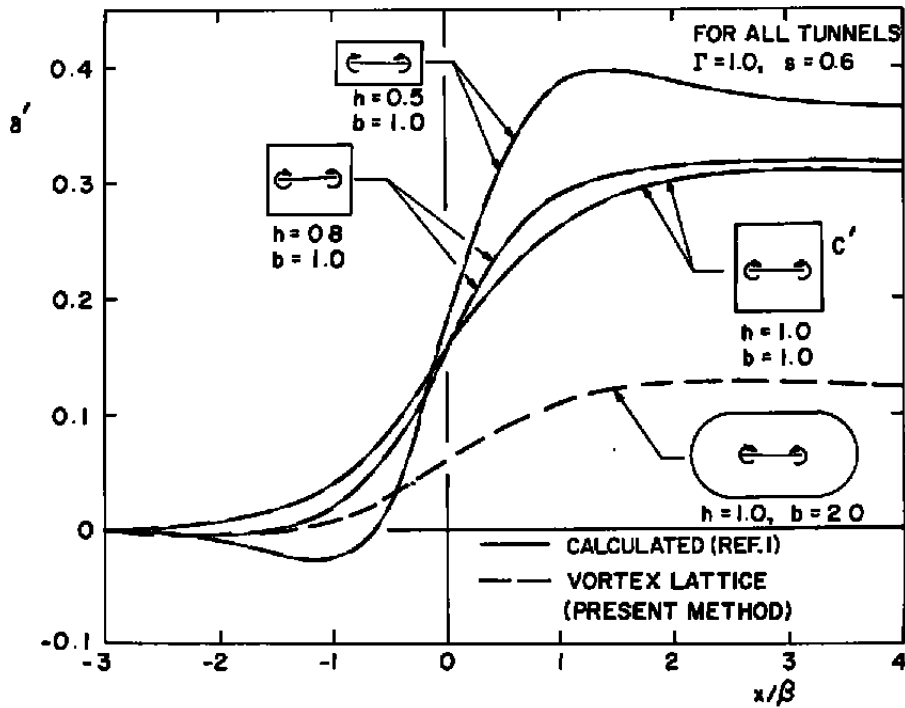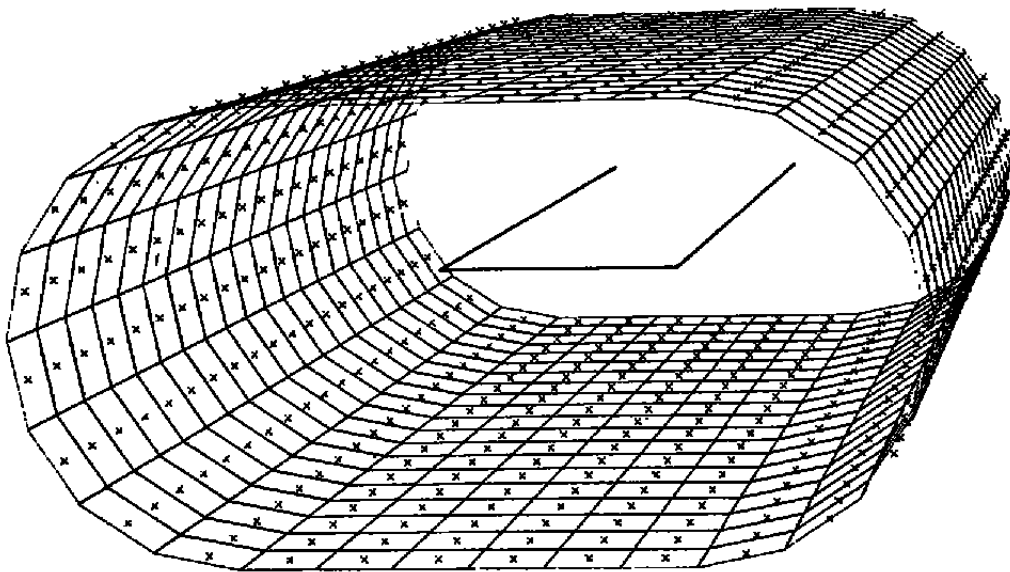Figure 3. Vortex lattice representation of the NASA/Ames flat oval tunnel.

7

Replacement of the closed wall with the appropriate boundary condition would permit calculations similar to those presented above for wind tunnels with slotted walls. The development of the necessary boundary condition is described in the following sections. Details of the numerical method used to obtain solutions are documented in Ref. 11.

2.1 SOLID SURFACES

The vortex lattice method uses an arrangement of vortex singularities to define solid bodies and other geometrical forms such as those illustrated in Figs. 1 and 3. For each vortex element of strength, Γ_i, one boundary condition may be specified at a point (control point) in the field. Generally a control point is located at the centroid of each vortex ring or horseshoe. To define a solid body surface the boundary condition imposed at each control point restricts the local induced velocity so that it is parallel to the surface at that point.

The numerical method involves describing the vortex network with a system of linear equations which are solved for the vortex strengths.

For a general system of vortex elements, the velocity at the ith control point is, from Ref. 11,

$$\vec{V}_i = \vec{V}_\infty + \vec{V}_{Vi} = \vec{V}_\infty + \sum_{j=1}^{N} \Gamma_j \, \vec{C}_{ij} \tag{3}$$

where $\vec{V}_\infty$ is the free-stream velocity and $\vec{V}_{Vi}$ is the velocity induced at the control point by the vortex system. The influence coefficient, $\vec{C}_{ij}$, is the velocity induced at the ith control point by the jth singularity when its strength is unity.

The most common form of boundary condition used in the vortex lattice method is

$$\vec{V}_i \cdot \hat{b}_i = G_i \tag{4}$$

To satisfy the expression at the ith control point the component of the local velocity, V_i, in the direction parallel to the unit normal vector, $\hat{b}_i$, must have a magnitude, G_i. For a solid boundary the velocity normal to the surface is zero. Combining Eqs. (3) and (4) yields, for all control points,

$$\vec{V}_i \cdot \hat{b}_i = \hat{V}_\infty \cdot \hat{b}_i + \sum_{j=1}^{N} \left(\vec{C}_{ij} \cdot \hat{b} \right) \Gamma_j = 0_{i=1,2...N} \tag{5}$$

Rearranging,

$$\sum_{j=1}^{N} \left(\vec{C}_{ij} \cdot \hat{b}_i \right) \Gamma_j = -\vec{V}_\infty \cdot \hat{b}_{i, i=1,2...N} \tag{6}$$

The set of N linear simultaneous homogeneous equations can be solved to yield the singularity strengths (Γ_i, i = 1,2 . . . N).

The velocity at any point, F, in the flow field can then be calculated as follows. Influence coefficients for the particular point are determined by using the Biot-Savart equation to compute the velocity induced by the straight line segment vortices of each vortex loop. Combining the influence coefficients provides a matrix, $\vec{C}_{Fj}$, which can be substituted into Eq. (3), yielding

$$\vec{V}_F = \vec{V}_\infty + \sum_{j=1}^{N} \Gamma_j \vec{C}_{Fj} \tag{7}$$

The pressure coefficient can be computed at the same point, using

$$C_{pF} = 1 - \left| \left(\vec{V}_F \middle/ \left| \vec{V}_\infty \right| \right) \right|^2 \tag{8}$$

Computation of either velocity or pressure coefficient in the immediate vicinity of the vortex sheet requires special consideration because of the close proximity of the finite singularities. Representative surface velocities are available only at the control points since the surface boundary condition is not satisfied elsewhere.

In determining the velocity on either side of the surface at a control point, one must account for the velocity jump across the discontinuity sheet. The jump velocity is equal to the cross product of the vortex sheet density vector, $\vec{K}_i$, and the unit vector normal to the local surface. The sign convention is illustrated graphically in Fig. 4. For the ith control point the difference between the outer and inner surface velocities can be written

$$\vec{V}_{Di} = \vec{K}_i \times \hat{B}_i \tag{9}$$

The unit vector, $\hat{B}_i$, is a special case of the unit normal, $\hat{b}_i$, and is included to define the sign of the velocity change. Due to the discrete nature of the lattice-type model, some care must be taken to evaluate the vortex sheet density, $\vec{K}_i$. A technique similar to

9

the one described by Rubbert in Ref. 12 was used in this study. The procedure involves dividing each individual vortex filament adjacent to the control point by an appropriate length to yield a density. The individual densities are averaged to provide an effective local sheet density in terms of the unknown singularity strength, Γ_i.
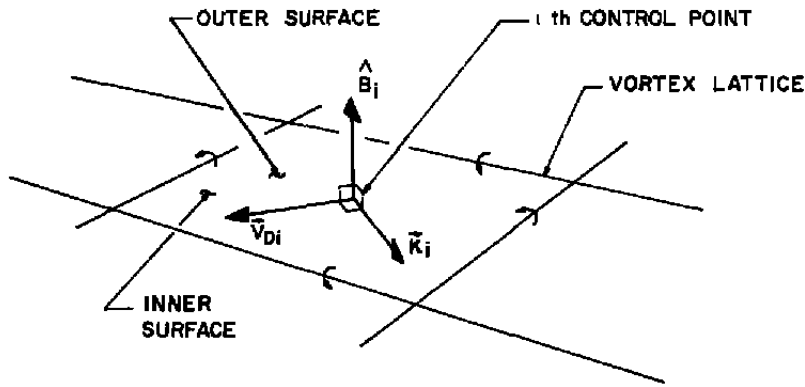
a. **Vector sign convention**
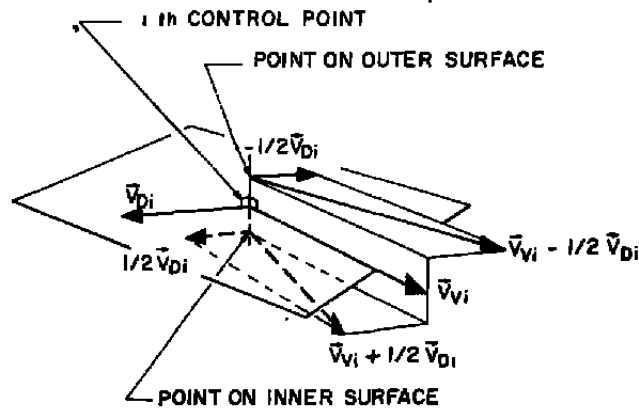
b. **Application of velocity correction**
Figure 4. Graphic representation of the jump
velocity correction technique.

The velocity can be determined on the inner side of the singularity sheet by adding one half of the jump velocity from Eq. (9) to the velocity induced by the free stream and the vortex network from Eq. (3). The inner and outer surface velocity at the ith control point, respectively, can be written as

$$\vec{V}_{IS_i} = \vec{V}_\infty + \vec{V}_{Vi} + \tfrac{1}{2}\vec{V}_{Di} = \vec{V}_\infty + \sum_{j=1}^{N} \Gamma_j \vec{C}_{ij} + \left(\tfrac{1}{2}\vec{K}_i \times \hat{B}_i \right) \qquad (10)$$

and

$$\vec{V}_{OS_i} = \vec{V}_{\infty} + \vec{V}_{Vi} - \tfrac{1}{2}\vec{V}_{Di} = \vec{V}_{\infty} + \sum_{j=1}^{N} \Gamma_j \vec{C}_{ij} - \left(\tfrac{1}{2}\vec{K}_i \times \hat{B}_i \right) \qquad (11)$$

Figure 4b graphically illustrates the vector addition of the jump velocity correction to the velocity induced by the vortex system. The free-stream velocity has been omitted for clarity.

The inner and outer surface pressure coefficients can now be calculated by substituting the velocities from Eqs. (10) and (11), respectively, into Eq. (8).

2.2 PERFORATED WALLS

Several theoretical boundary condition formulations have been developed for dealing with various wind tunnel wall configurations. Of primary interest are those discussed in Refs. 1 through 4 for representing homogeneous perforated and slotted boundaries. The interference results for rectangular tunnels with ventilated upper and lower walls and closed side walls have been used throughout the present study for comparison with existing theoretical calculations. In each case a single horseshoe vortex of unit strength was utilized to represent the lifting model.

The perforated wall boundary condition presented in Ref. 2 is intended to represent a tunnel wall with a uniform distribution of holes. The theory was developed based upon an assumption that such a wall behaved in the same manner as a porous material boundary (i.e., that the flow through the surface was linearly proportional to the pressure difference across the boundary). The boundary condition can be written as follows:

$$\frac{\partial \phi}{\partial x} + C \frac{\partial \phi}{\partial n} = 0 \qquad (12)$$

Expressed in terms of the velocity on the top wall of a wind tunnel, Eq. (12) becomes

$$u + Cw = 0 \qquad (13)$$

The boundary condition states that the perturbation velocity components at the wall are related by a constant, C. The wall porosity parameter, Q, is conventionally defined as

$$Q = 1/(1 + C) \qquad (14)$$

For a closed wall where $Q = 0$ (or $C = \infty$), Eq. (13) reduces to

$$w = 0 \tag{15}$$

For $Q = 1$ (or $C = 0$) the boundary condition represents a constant pressure or open jet boundary when

$$u = 0 \tag{16}$$

The form of the perforated wall boundary condition is similar to that used for the solid surface [Eq. (4)].

Equation (13) states that the velocity in a particular direction $(\hat{i} + C\hat{k})$ must be zero along the top wind tunnel wall. As was the case with the solid boundary, the scalar velocity, G_i, is set equal to zero. The unit normal vector, $\hat{b}_i$, in Eq. (4) is replaced by a unit vector, $\hat{d}_i$, in a direction determined by the wall porosity. For an upper tunnel wall the new unit vector can be written

$$\hat{d}_i = \frac{\hat{i}}{\sqrt{1 + C^2}} + \frac{C\hat{k}}{\sqrt{1 + C^2}} \tag{17}$$

The solid surface formulation dealt only with restricting the velocity in the direction normal to the surface. With the introduction of the other component (i.e., the direction $\hat{k}$), it becomes necessary to account for the effects of local singularity sheet density. The velocity expression developed for computing the velocity on the inner surface at a control point, Eq. 10, was used since it contains the required terms. The perforated wall boundary condition on the inner surface of a vortex lattice wind tunnel becomes

$$\vec{V}_{IS} \cdot \hat{d}_i = 0 \tag{18}$$

The boundary condition is applied to Eq. 10, yielding, for the ith control point,

$$\vec{V}_{IS_i} \cdot \hat{d}_i = \vec{V}_\infty \cdot \hat{d}_i - \sum_{j=1}^{N} \left(\overline{C}_{ij} \cdot \hat{d}_i \right) \Gamma_j - \left(\tfrac{1}{4}\vec{K}_i \times \hat{B}_i \right) \cdot \hat{d}_i = 0 \tag{19}$$

Evaluating the terms in Eq. (10) for each of the control points at which the perforated boundary condition is to be imposed (i.e., $i = 1, 2, \ldots N_p$) yields N_p linear simultaneous equations in terms of the N unknown Γ_j values. The remaining equations, if $N_p \neq N$, may represent solid surface control points on nonperforated portions of the tunnel wall or on the test article.

Comparisons of centerline wall interference distributions from Refs. 1 and 3 with data calculated using the vortex lattice model are presented in Fig. 5 for several porosity parameter values. The agreement of the vortex lattice results with solutions from available theoretical calculations is good.

2.3 SLOTTED WALLS

Early slotted wall models were based upon discrete geometric representations of slots and solid panels (Ref. 13). A typical example, presented in Fig. 6, has one wide slot in each corner of the cross section. The slots are simulated by vortex elements which are the same width as the slots. A free jet or constant pressure boundary condition is imposed at the slot control points to permit flow through the wall. The solid panels are represented by vortex loops with conventional closed wall boundary conditions specified at their centroids. The technique works well for tunnels with small numbers of large slots, as discussed in Ref. 13. For wind tunnels with several narrow slots a large number of vortex elements is required since the singularity spacing must be kept in the order of the slot width. This in turn places prohibitive demands upon the computer capability. Since most existing slotted tunnels were designed with narrow slots, the discrete simulation technique was abandoned.
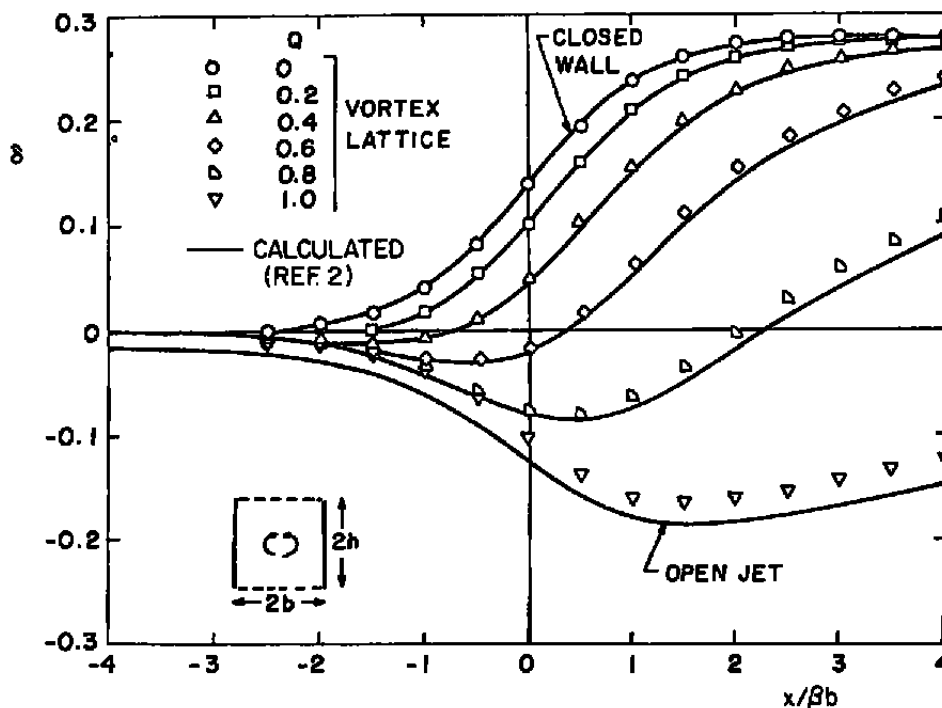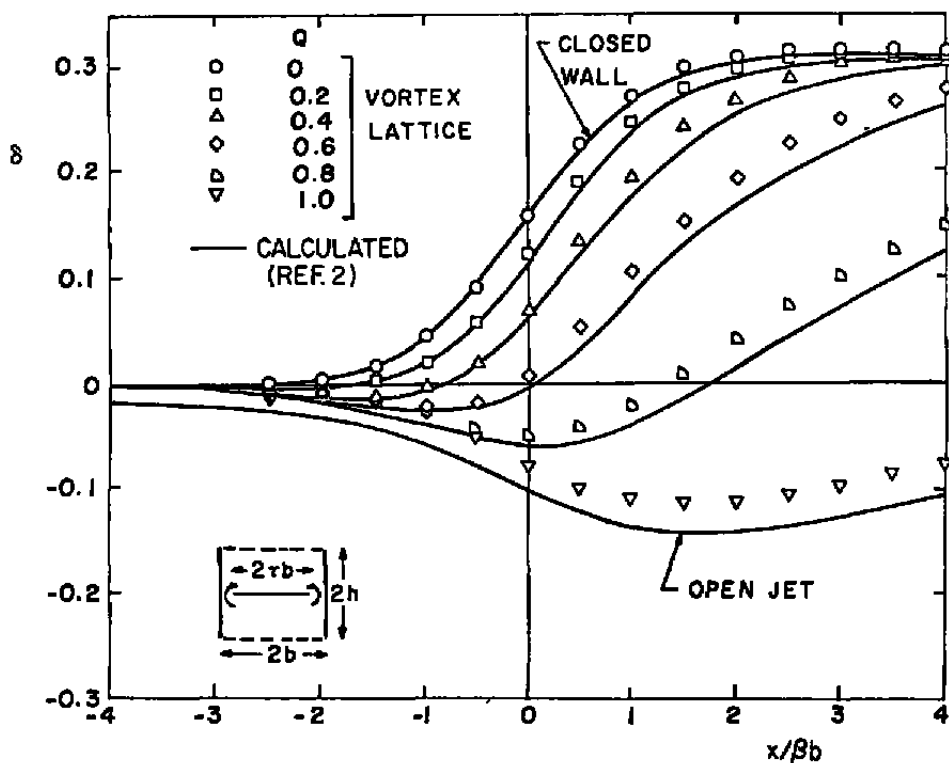

a. $\lambda = 1$, $\tau = 0.05$, solid side walls, top and bottom perforated

Figure 5. The vortex lattice solution and other calculated results for various perforated wall tunnels.
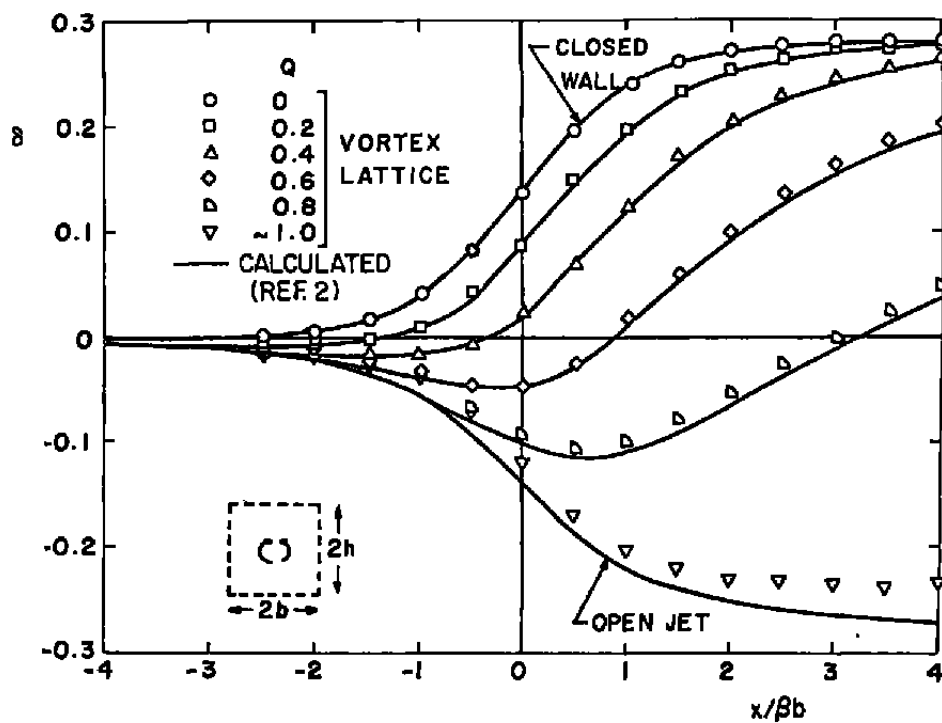
b. $\lambda = 1$, $\tau = 0.05$, all walls perforated

ç. $\lambda = 1$, $\tau = 0.6$, solid side walls, top and bottom perforated

Figure 5. Concluded.
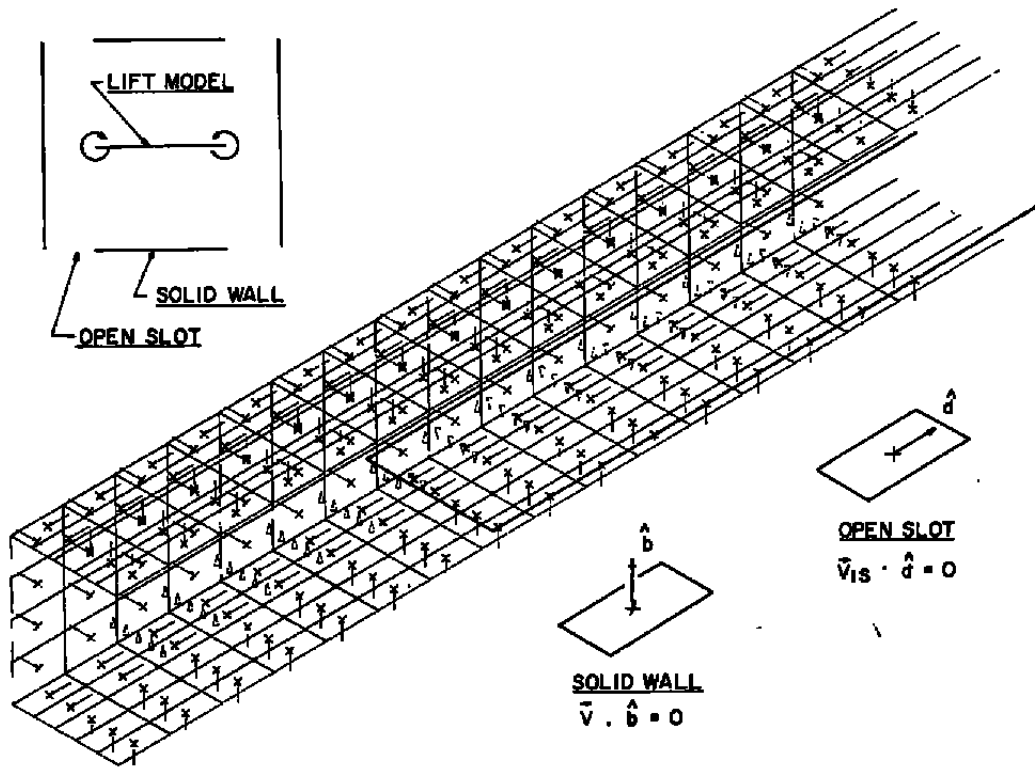
Figure 6. Vortex lattice representation of a wind tunnel with discrete slots.

The alternative method involved application of a homogeneous slotted wall boundary condition over the entire slotted wall. Such a boundary condition has been used by several investigators (e.g., Refs. 1, 5, 6, 7, 8, 9, and 10). The boundary condition attributed to Buseman in Ref. 6 can be expressed as

$$\frac{\partial \phi}{\partial x} + \kappa \frac{\partial^2 \phi}{\partial x \, \partial n} = 0 \qquad (20)$$

where x is the direction of the tunnel axis and n is outward, normal to the wall inner surface. The geometric slot parameter, κ, is related to the physical tunnel dimensions shown in Fig. 7 by Chen and Mears (Ref. 5) as

$$\kappa = \frac{d-a}{2} \tan \left[\frac{\pi}{2} \left(1 - \frac{a}{d} \right) \right] \qquad (21)$$

and

$$P = 1 / \left[1 - (\kappa/h) \right] \qquad (22)$$

15

LOOKING UPSTREAM
x - POSITIVE DOWNSTREAM
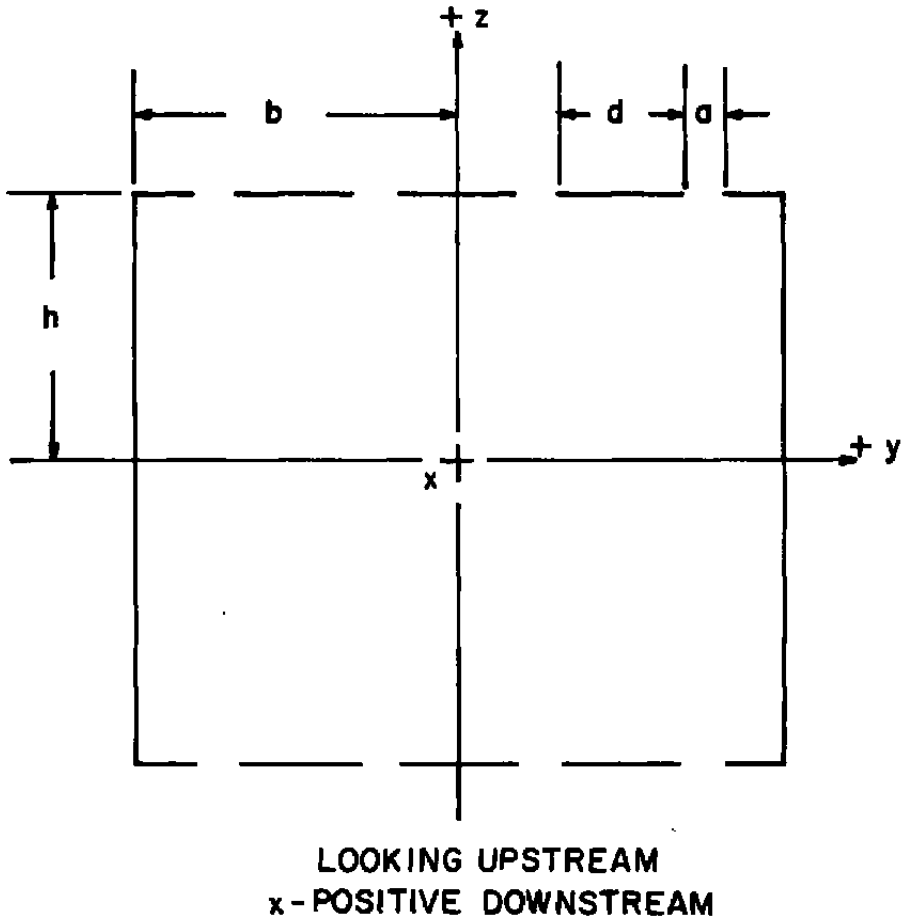
Figure 7. Slotted wall tunnel cross-sectional geometry and coordinate system.

The slot parameter, P, is most frequently used since its limiting values are 0 and 1 for closed and open jet boundaries, respectively, whereas κ varies from 0 to infinity.

Written in terms of the upper wind tunnel wall, the boundary condition becomes

$$u + \kappa \frac{\partial w}{\partial x} = 0 \qquad (23)$$

where $\partial w/\partial x$ is the local gradient of the w-component of velocity in the x-direction. Rewritten in terms appropriate for a discretized representation with a uniform singularity spacing, Δx, in the x-direction, the boundary condition at the ith control point is

$$u_i + \kappa \frac{\left(w_{i+1} - w_{i-1} \right)}{2\Delta x} = 0 \qquad (24)$$

16

Rearranging,

$$u_i + \kappa/2\Delta x \left(w_{i+1} - w_{i-1} \right) = 0 \tag{25}$$

Defining $\kappa^* = \kappa/2\Delta x$ yields

$$u_i - \kappa^* \left(w_{i+1} - w_{i-1} \right) = 0 \tag{26}$$

which is the form of Eq. (13). A unit direction vector analogous to Eq. (18) can be formulated as

$$\hat{e}_i = \frac{\hat{i}}{\sqrt{1 + \kappa^{*2}}} + \frac{\kappa^* \hat{k}}{\sqrt{1 + \kappa^{*2}}} \tag{27}$$

By the same analogy, a control vector expression is needed which is similar to the inner surface velocity vector in Eq. (10) but modified to contain the new parameters introduced by the slotted wall boundary condition. On the basis of the direction vector already defined in Eq. (27), such an expression can be written as

$$\vec{V}^*_{IS_i} = \vec{V}_\infty + \vec{V}^*_{V_i} + \tfrac{1}{2}\vec{V}_{Di} = \vec{V}_\infty + \sum_{j=1}^{N} \Gamma_j \, \vec{C}^*_{ij} + \left(\tfrac{1}{2}\vec{K}_i \times \vec{B}_i \right) \tag{28}$$

In terms of the wind tunnel upper wall, the vortex system induced velocity,

$$\vec{V}_{V_i} = u_i \, \hat{i} + v_i \, \hat{j} + w_i \, \hat{k} \tag{29}$$

has been replaced with a new vector,

$$\vec{V}^*_{V_i} = u_i \, \hat{i} + v_i \, \hat{j} + \left(w_{i+1} - w_{i-1} \right) \hat{k} \tag{30}$$

It is not necessary to alter the free-stream or jump velocity terms since neither has a component in the z-direction. The boundary condition can be written as

$$\vec{V}^*_{IS_i} \cdot \hat{e}_i = 0 \tag{31}$$

which yields

$$\vec{V}^{*}_{IS_{i}} \cdot \hat{e}_{i} = \vec{V}_{\infty} \cdot \hat{e}_{i} + \sum_{j=1}^{N} \left(\vec{C}^{*}_{ij} \cdot \hat{e}_{i} \right) \Gamma_{j} + \left(\tfrac{1}{2} \vec{K}_{i} \times \vec{B}_{i} \right) \cdot \hat{e}_{i} = 0 \qquad (32)$$

Evaluating Eq. (32) at each control point on the slotted walls and combining the resulting equations with those for other types of boundaries yields the usual set of N simultaneous linear equations in terms of the unknown vortex strengths, Γ_{j}.

Calculations were made for a basic slotted wind tunnel configuration similar to the one previously used in the perforated wall analysis. The test section was square in cross section with closed side walls and slotted upper and lower walls. Lift was generated by a single horseshoe vortex. Results of the computations are presented in Fig. 8 along with analytic solutions from Ref. 3. As can be seen, correlation is excellent throughout the slot parameter range.
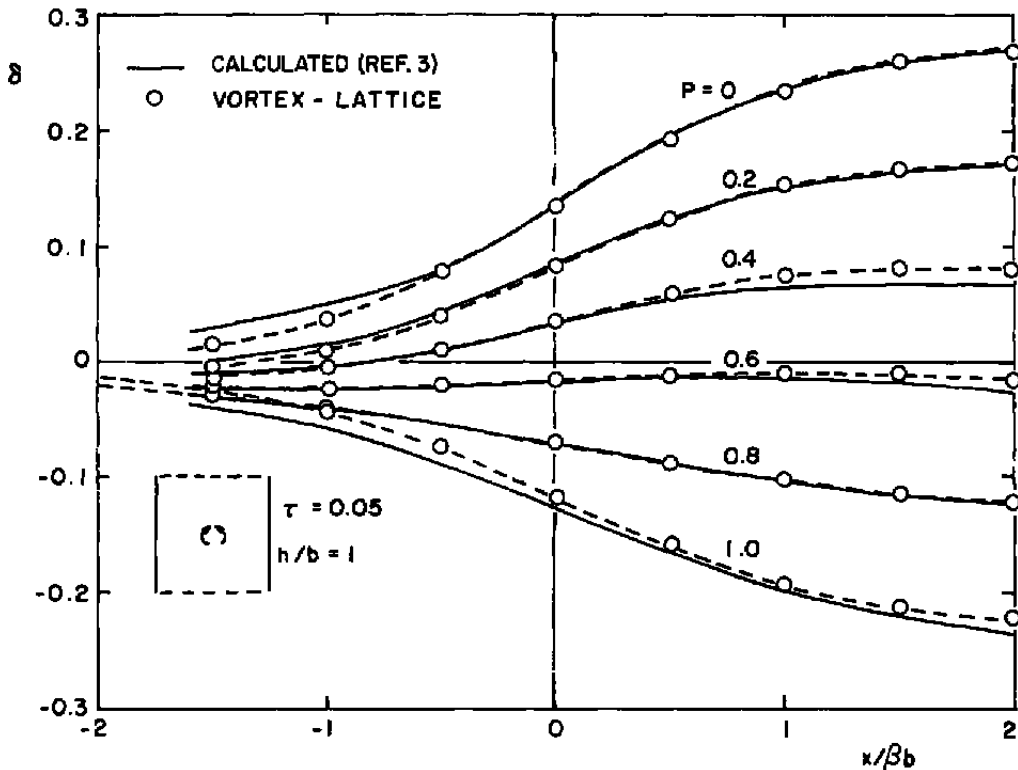

Figure 8. The vortex lattice solution and other calculated results for several values of the homogeneous slot parameter, P.

3.0 APPLICATION OF THE METHOD

The vortex lattice method can predict lift interference in tunnels with closed, perforated, or slotted walls for lifting models (Figs. 5 and 8). The configurations presented thus far have been limited to those involving an elementary horseshoe vortex of fixed strength to represent test article lift. The method is equally valid for a model with distributed lift. Since the formulation is linear, additional specified vortex elements of fixed strength can be included to represent the desired lift distribution. Calculations can readily be performed for test article configurations so complex that analysis by other means is impractical.

The vortex lattice technique is also capable of accounting for the mutual interaction between the wind tunnel walls and the test article. The requirement of the fixed strength lifting element distribution can be relaxed and replaced with a set of boundary conditions and vortices of unspecified strength. The solution, obtained by simultaneously satisfying the tunnel wall and test article boundary conditions, contains influence of both the tunnel and the test article. The tunnel wall effects can be assessed directly through a comparison of the mutual interference results and the solution obtained in an infinite free stream (i.e., an interference-free environment). The following sections demonstrate the use of unspecified strength vortices to represent the test article.

3.1 DISTRIBUTED LIFT MODEL

A more realistic model than the simple horseshoe vortex model was selected to investigate the compatibility of the ventilated wall boundary conditions with a distributed lift model represented by unknown strength vortex elements.

Dimensions of the wing-tail configuration selected are shown in Fig. 9. The vortex lattice representation of the lifting model is shown in Fig. 10 installed in the 30- by 45-in. vortex lattice wind tunnel used in the investigation. The test section represents a low speed wind tunnel at AEDC having the same dimensions.

The wing model is divided into six sections along the span. Each section is made up of 200 vortex elements, distributed chordwise over the airfoil surface, with 100 on the upper surface and 100 on the lower surface. Both the vortices and control points are distributed by a cosine function to provide closer spacing near the leading and trailing edges. The unit normal vectors located at the control points are illustrated in the same figure along with a detail of the wingtip vortex elements. The vortex lattice model of the tail was essentially the same as the wing except for scale.
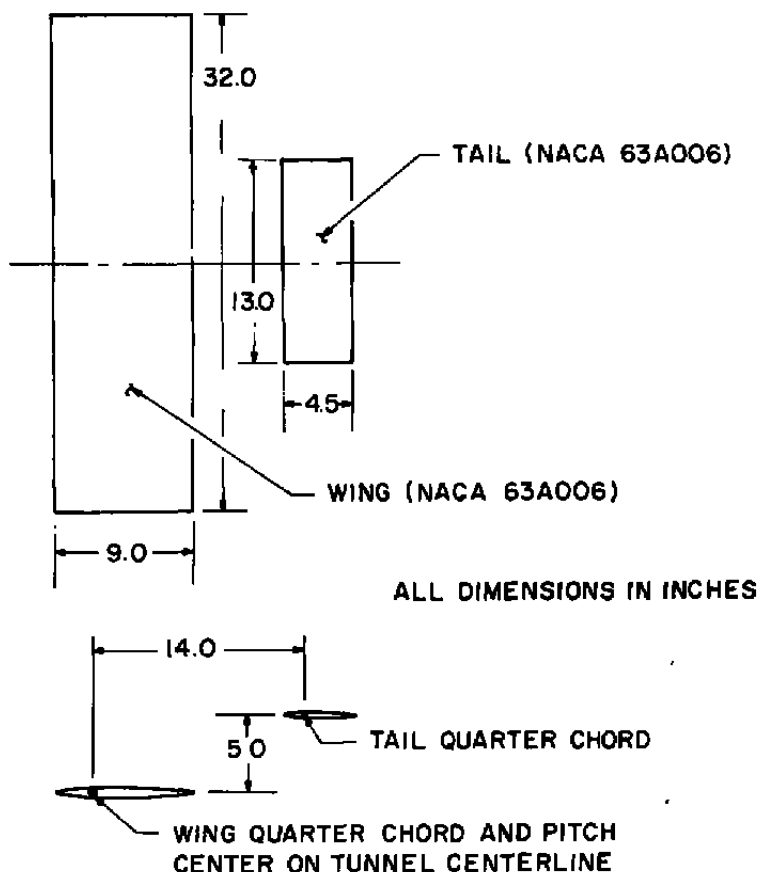
Figure 9. Dimensions of the lifting model.

The wind tunnel is represented by equally spaced rows of vortex elements oriented parallel to the tunnel axis, with six rows on both the upper and lower walls and four on each side wall. All four walls were modeled to permit selection of either the closed or slotted boundary condition.

3.2 WING/TAIL PRESSURE DISTRIBUTIONS

The chordwise distribution of pressure coefficient was calculated for the upper and lower surfaces of the vortex lattice wing and tail representations.

The interference-free pressure distributions are presented in Fig. 11 for five incidence angles to illustrate the effect of angle-of-attack variation. A comparison of the $a = 2$ and -2 deg data indicates that the vertical asymmetry of the wing/tail configuration had only a slight effect on the tail pressure distribution. The effect on the wing pressures was almost undetectable.
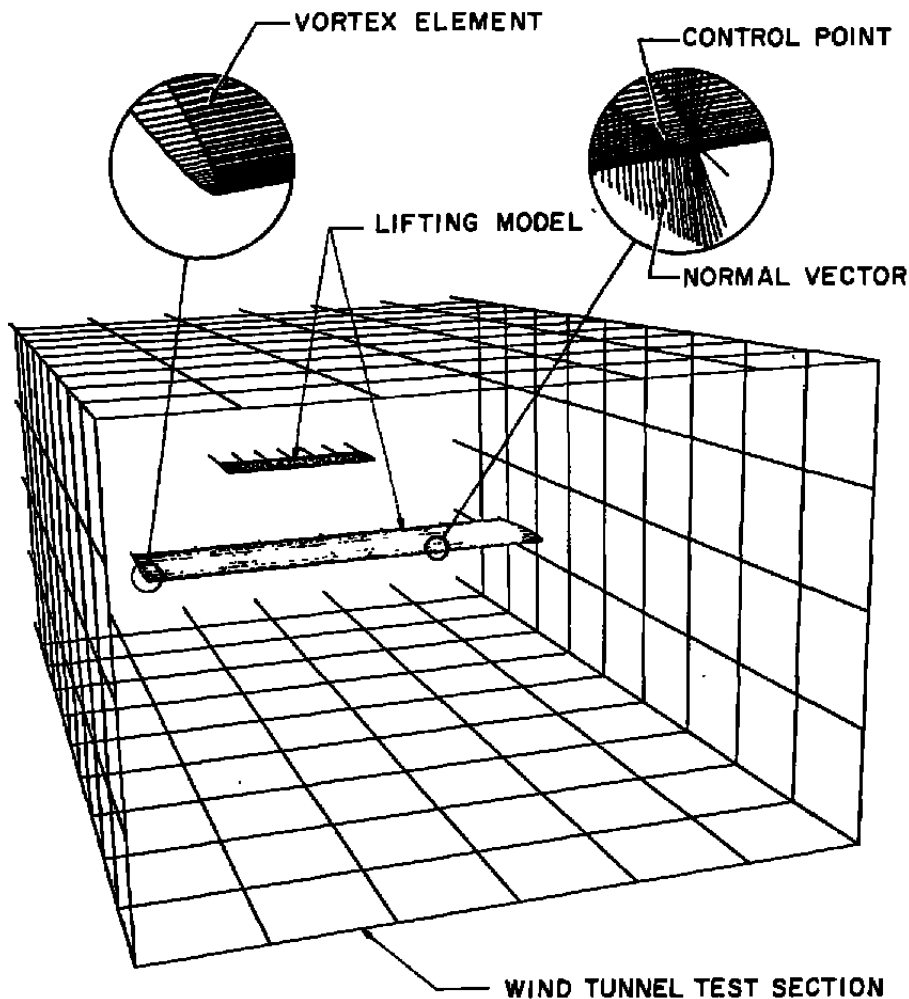
Figure 10. Vortex lattice representation of a wind tunnel/lifting model.

Three variations of the Fig. 10 configuration were investigated, namely the lifting model in a free stream (with no tunnel), the lifting model in a closed tunnel, and the lifting model in a tunnel with closed side walls and slotted upper and lower walls. In all three cases pressures were obtained at the quarter-span location of each lifting surface. The resulting pressure distributions, computed at $\alpha = 6$ deg, are presented in Fig. 12. As expected, the effect of the closed wall test section was to increase the upper surface velocities and to decrease those on the lower surface of both the wing and tail. Thus, the upper surface pressure coefficients are more negative for the closed wall case than those in the free stream. Since the lower surface pressures become more positive (or less negative over part of the tail), a net increase in the lift coefficient would result. The overall effect on the pressure distributions caused by confinement of the flow field within the solid boundaries appears to be equivalent to that resulting from an increase in

the model angle of attack. Such an effect is consistent with theory (Refs. 1 and 3), which predicts a positive interference in the vicinity of a single concentrated lift disturbance in a closed tunnel. The interference upwash velocity distribution was computed using the vortex-lattice closed wall tunnel and wing/tail models. The results, presented in Fig. 13, show that a positive upwash is also generated at both the wing and tail locations for the distributed lift case.

Pressure distributions computed within the 30- by 45-in. wind tunnel with slotted upper and lower walls and closed side walls are also presented in Fig. 12. A slotted wall
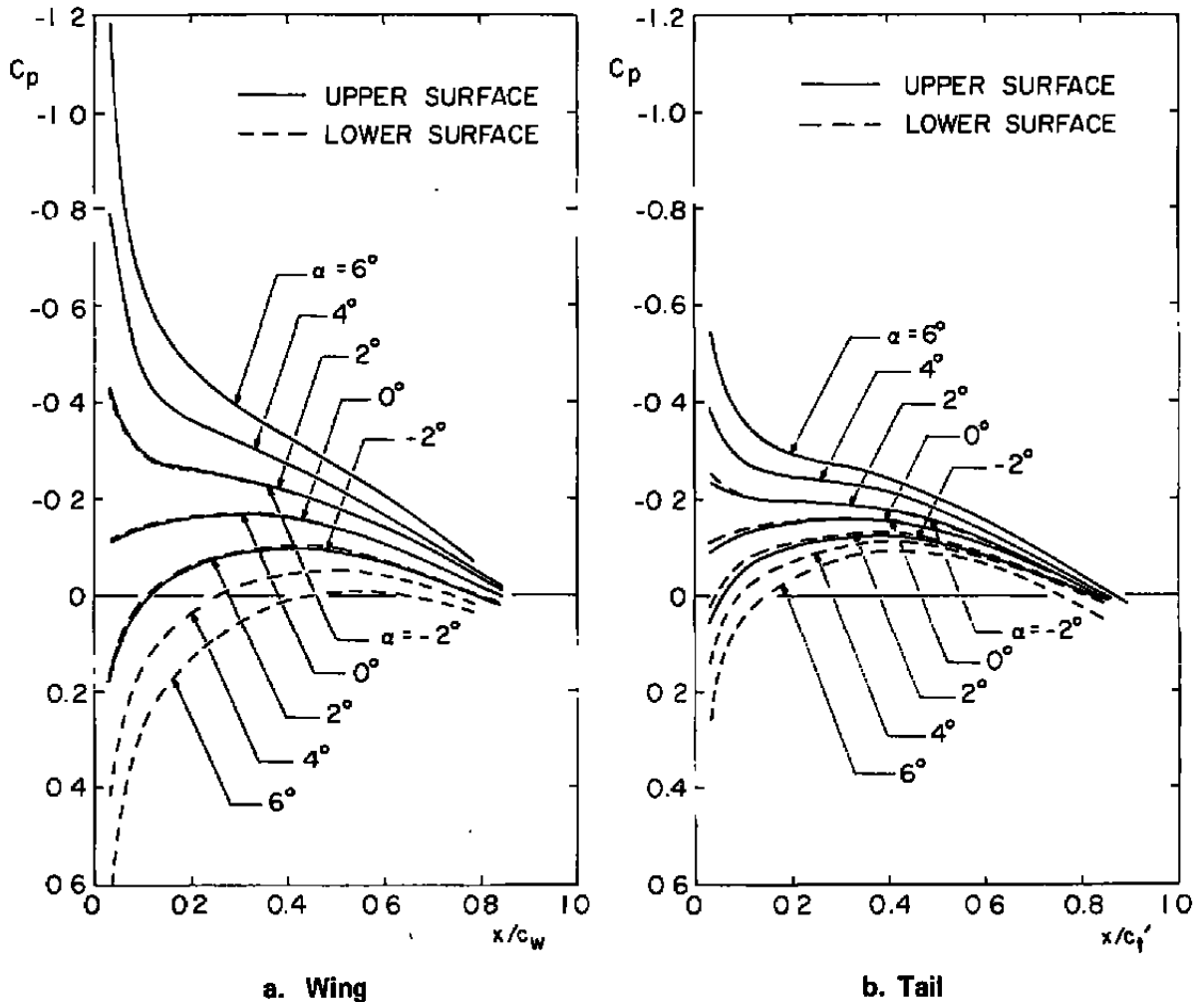

a. Wing   b. Tail

Figure 11. Pressure distributions for the wing/tail model computed in a free stream.

parameter value, P = 0.4, was used in the computations. The value, based on Ref. 3, was selected to provide minimum wall interference on the wing. The excellent agreement of the calculations for the wing in the slotted tunnel with the free-stream solution (Fig. 12a) indicates that the interference induced by the walls was small at the wing location. A similar comparison of the tail pressure distributions (Fig. 12b) reveals, however, that the data do not correlate as well. It appears that the slotted wall provided too much flow relief, resulting in an over-correction in the region of the tail.
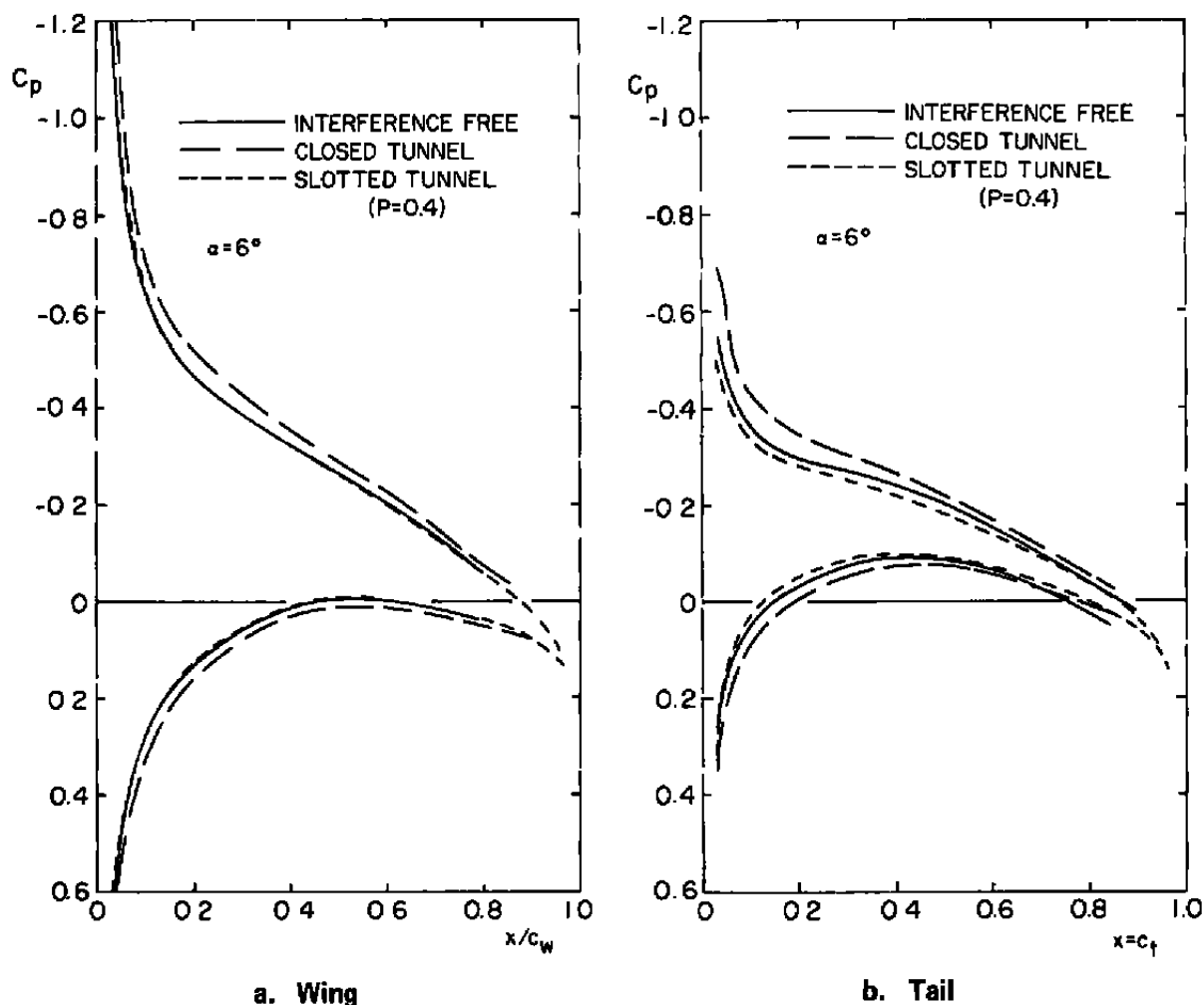

a. Wing   b. Tail

Figure 12. Pressure distributions for the wing/tail model computed in a free stream and in a 30- by 45-in. tunnel.
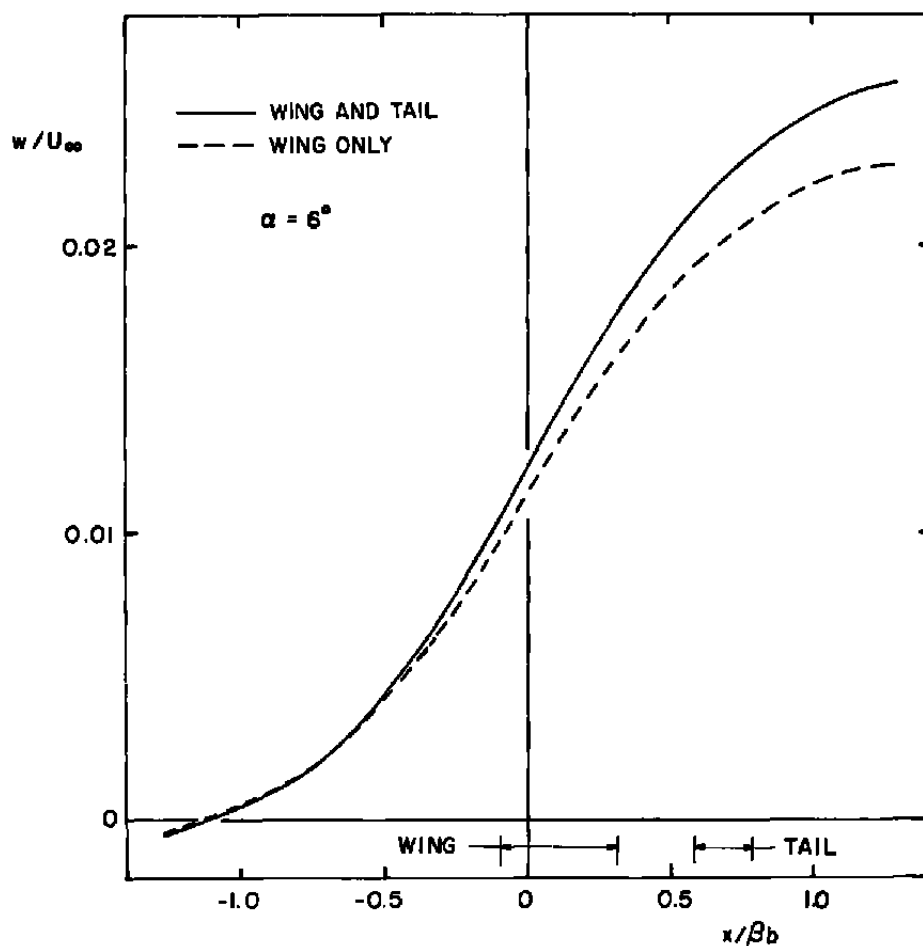
Figure 13. Normalized upwash velocity computed along the centerline of a 30- by 45-in. tunnel with closed walls.

4.0 CONCLUDING REMARKS

A vortex lattice technique for simulating the effects of perforations and longitudinal slots in wind tunnel walls has been evaluated. The lift interference factor, δ, was computed for a single lifting element in several basic wind tunnel configurations. Good correlation has been shown between the vortex lattice results and other theoretical calculated solutions. The method was also applied to a test article having distributed lift. The wing/tail configuration, represented by an arrangement of boundary conditions and vortices of unknown strength. is described. Computed wind tunnel wall effects on the lifting model pressure distribution appear reasonable.

Coupled with the ability of the vortex lattice technique to accurately represent conventional test articles, the ventilated boundary condition formulation has provided a powerful tool for predicting the influence of most perforated or slotted wind tunnel configurations.

REFERENCES

1. Kraft, E. M. "Upwash Interference on a Symmetrical Wing in a Rectangular Ventilated Wall Wind Tunnel: Part I, Development of Theory." AEDC-TR-72-187 (AD757196), March 1973.

2. Lo, C. F. and Oliver, R. H. "Boundary Interference in a Rectangular Wind Tunnel with Perforated Walls." AEDC-TR-70-67 (AD704123), April 1970.

3. Pindzola, M. and Lo, C. F. "Boundary Interference at Subsonic Speeds in Wind Tunnels with Ventilated Walls." AEDC-TR-69-47 (AD687440), May 1969.

4. Kraft, E. M. and Lo, C. F. "A General Solution for Lift Interference in Rectangular Ventilated Wind Tunnels." AIAA Journal, Vol. 11, No. 10, October 1973, pp. 1365-1366.

5. Chen, C. F. and Mears, J. W. "Experimental and Theoretical Study of Mean Boundary Conditions at Perforated and Longitudinally Slotted Wind Tunnel Walls." AEDC-TR-57-20 (AD144320), December 1957.

6. Davis, D. D., Jr. and Moore, D. "Analytical Study of Blockage and Lift-Interference Corrections for Slotted Tunnels Obtained by the Substitution of an Equivalent Homogeneous Boundary for the Discreet Slots." NACA RM L53E07B, June 1953.

7. Wright, R. H. and Barger, R. L. "Wind Tunnel Lift Interference on Sweptback Wings in Rectangular Test Sections with Slotted Top and Bottom Walls." NASA TR R-241, June 1966.

8. Wright, R. H. and Keller, J. D. "Wind Tunnel Lift Interference on Sweptback Wings in Rectangular Test Sections with Slotted Side Walls." NASA TR R-344, July 1970.

9. Baldwin, B. S., et al. "Wall Interference in Wind Tunnels with Slotted and Porous Boundaries at Subsonic Speeds." NACA TN 3176, May 1954.

10. Barnwell, R. W. "Improvements in the Slotted-Wall Boundary Condition." Proceedings of the AIAA 9th Aerodynamic Testing Conference, Arlington, Texas, June 1976, pp. 21-30.

11. Todd, D. C. and Palko, R. L. "The AEDC Three-Dimensional, Potential Flow Computer Program." AEDC-TR-75-75, Vols. I (ADA021693) and II (ADA021694), February 1976.

12. Rubbert, P. E. "Theoretical Characteristics of Arbitrary Wings by a Non-Planar Vortex-Lattice Method. "Boeing Company Document DG-9244, The Boeing Company, Seattle, Washington, August 1967.

13. Heltsley, F. L. "Report on the Status of a Slotted Wind Tunnel Wall Representation Using the Vortex Lattice Technique." Proceedings of Vortex Lattice Utilization Workshop, May 17-18, 1976. NASA SP-405, pp. 145 and 162.

NOMENCLATURE

a   Slot width, ft

.b   Tunnel half width, ft

$\hat{B}_i$ Unit normal vector at the ith control point, negative away from the boundary on the inner surface

$\hat{b}_i$ Unit normal vector at the ith control point, unit control vector

C   Wind tunnel cross-sectional area, ft^2; constant related to wall porosity, Eq. (12)

C'   Cross-sectional area of a reference wind tunnel where h = 1 and b = 1, ft^2

C_{ij} Influence coefficient matrix, velocity induced at the ith control point by the jth singularity when its strength is unity

C_L Lift coefficient, C_L = Lift/(q_∞ S)

C_p Pressure coefficient, Eq. (8)

c   Mean chord, ft

d   Slot spacing, ft

$\hat{d}_i$ Unit vector at the ith control point with direction related to wall porosity, Eq. (17)

$\hat{e}_i$ Unit vector at the ith control point with direction related to the slot parameter, Eq. (27)

G_i	Magnitude of the component of velocity at the ith control point parallel to the local unit control vector, Eq. (4)
h	Wind tunnel half height, ft
$\hat{i}, \hat{j}, \hat{k}$	Unit velocity vector components related to the x,y,z coordinates, respectively
$\vec{K}_i$	Vortex sheet density vector, Eq. (9)
M	Mach number
N	Number of independent linear equations: number of singularities of unknown strength
n	Coordinate normal to the local boundary, positive out, Eq. (12)
P	Homogeneous slot parameter, $1/[1(k/h)]$
Q	Porosity parameter, $1/(1 + C)$
q_∞	Free-stream dynamic pressure, psf
S	Wing area, ft^2
s	Wing semispan, ft
u,v,w	Velocity component magnitudes related to the x,y,z coordinates, respectively, ft/sec
$\vec{V}$	Velocity vector, ft/sec
x	Coordinate along tunnel axis, positive downstream, ft
y	Horizontal coordinate across tunnel, positive left looking downstream, ft
z	Vertical coordinate, positive up, ft
α	Angle of attack, positive up, deg
β	Compressibility factor, $(1 - M_\infty^2)^{\frac{1}{2}}$
Γ	Vortex strength density, ft/sec
Δx	Vortex lattice spacing in the x-direction, ft

δ	Wall interference factor
δ'	Modified wall interference factor, $\delta(C'/C)$
κ	Geometric slot parameter, Eq. (20)
κ^*	Modified geometric slot parameter, $\kappa^* = \kappa/2\Delta x$
λ	Tunnel height-to-width ratio, h/b
τ	Wingspan-to-tunnel width ratio, s/b
ϕ	Velocity potential

SUBSCRIPTS

D	Discontinuity
F	General point in the field
i,j	Indices
IS	Inner surface
OS	Outer surface
P	Perforated wall, pressure
t	tail
V	Vortices
w	Wing
∞	Free stream

SUPERSCRIPTS

$'$	Related to C'
$*$	Based on κ^*